High degree oscillations in 3D numerical simulations of solar convection

By D. Georgobiani, R.F. Stein †, Å. Nordlund ‡, A.G. Kosovichev ¶
AND N.N. Mansour

1. Motivation and objectives

High-degree acoustic modes probe shallow solar layers, where convection drives oscillations. We study these oscillations by means of the three-dimensional hydrodynamic code of Nordlund & Stein (1990). The code simulates a small part of the solar convection zone, and is therefore suitable for studies of high degree modes. In our previous work Georgobiani *et al.* (2000), we looked at the modes with angular degree $\ell = 740$. However, these modes in the Sun are reflected at 9-10 Mm beneath the surface, but the simulated domain was too shallow to include their lower turning points. As a result, the mode frequencies did not match the observed ones, although the velocity amplitudes were quite similar.

In this work, we study modes of higher degree, $\ell = 1480$. These modes have their lower turning points around 3 Mm, and therefore their eigenfunctions fit inside the simulated box. We compare these modes with the observed oscillations of the same angular degree. We find a good match in their power spectra, except for the noise level at very low frequencies. Frequencies, amplitudes and widths of the modes match rather well. Similarity of mode line asymmetries and widths in observations and simulations suggests that mode excitation and damping mechanisms are correctly captured in the simulations.

We also compare spectra of full-disk and high-resolution solar observations, trying to establish a link between power spectral densities in observational data sets of different spatial resolution, in order to facilitate their comparison with the simulated data.

This work is organized as follows: Section 2 describes the simulation code; Section 3 presents the two sets of the SOHO/MDI data analyzed in our work; Section 4 outlines the procedure for calculating the power spectra; Section 5 is devoted to the results, followed by a discussion and a description of our future plans.

2. Numerical model

To simulate a small region of the upper solar convection zone, we use the 3D radiative–hydrodynamic (RHD) code by Stein and Nordlund (for a detailed description, see Stein & Nordlund (2000) and references therein). The code solves a complete system of hydrodynamic equations. It has a detailed radiative transfer treatment, thus properly represents both convection and radiation in the upper convection zone and the photosphere. The detailed radiative model in the code is very important for studies of solar oscillations. The computational domain is 3 Mm deep, starting from near the temperature minimum

† Department of Physics and Astronomy, Michigan State University, Lansing, MI 48824, USA
‡ Niels Bohr Institute for Astronomy, Physics and Geophysics, Juliane Maries Vej 30, DK–2100 Copenhagen, Denmark
¶ Hansen Experimental Physics Laboratory, Stanford University, Stanford, CA 94305, USA

at 0.5 Mm above the $\tau = 1$ surface, and extending to 2.5 Mm beneath it. The horizontal area of the domain is 6 Mm × 6 Mm. The horizontal resolution is 100 km, while the vertical one varies from 35 to 70 km, depending on the height (superadiabatic region is resolved better than the convective zone). The number of mesh points was 63 × 63 × 63. Three-dimensional snapshots of several physical properties (velocity, temperature, density, internal energy) are recorded every 30 seconds, and the total simulation sequence spans 72 hours of solar time.

To compare our results with SOHO/MDI observations, for each time step we extract 2D horizontal planes of the vertical velocity component at approximately 200 km above the visible surface ($\tau = 1$). This level approximately corresponds to the height of the NiI 6768 line formation, in which the observations are taken.

3. Observed velocity data

The SOHO/MDI Doppler velocity data used for comparison are simultaneous high-resolution (0.6 arcsec/pixel) and full-disk (2 arcsec/pixel) images taken on June 14 - 16, 1997. The high-resolution sub-region of 62.5 Mm × 62.5 Mm (128 × 128 pixels) was tracked with solar rotation for 2.5 days. The full-disk data spans 3 days. In both data sets, the time interval between the images is 1 minute. The high-resolution data represent a patch of the solar surface, therefore, after removing the solar rotation, we can apply the same spectral analysis as the one we use for the simulated velocity data. The full-disk data underwent spatial filtering in terms of spherical harmonic transform, and are available for different values of angular degree ℓ, from 0 to 1000, and corresponding azimuthal orders $m = -\ell, ..., \ell$. We used these data for $\ell = 740$, to compare with the high-resolution data, and also for $\ell = 370$, to see how the oscillation power might scale with angular degree.

4. Power spectra calculations

To calculate the velocity power spectrum for the simulated data, we perform spatial filtering using harmonic functions of horizontal coordinates on the 2D surfaces of vertical velocity at each time step, take Fourier transform in time and multiply by its conjugate. The horizontal spatial filtering allows us to extract modes corresponding to a given angular degree. Horizontal averaging extracts radial modes, while filtering with spatial sines and cosines of different horizontal wavenumbers gives non-radial modes. For waves with horizontal wavelength $L = 6$ Mm (the box size), the horizontal wavenumber is $k_h = 2\pi/L \simeq 1$ Mm^{-1}, and their angular degree is $\ell \simeq k_h R \simeq 740$, where R is the solar radius; for waves with $L = 3$ Mm (half the box size), $k_h \simeq 2$ Mm^{-1}, and $\ell \simeq 1480$ (for more details, see Georgobiani *et al.* (2000)). These are the modes we are especially interested in, because we expect them to be captured within the simulated domain.

In non-radial cases, we get the spectra for four spatial filters (sine and cosine in x and y direction), and then perform summation over these spectra. We remove the solar rotation trend from the high-resolution SOHO/MDI data and perform similar spectral analysis. For the full-disk data, we also remove the effect of solar differential rotation for different m by imposing frequency shifts according to the solar rotation law, and then sum over $m = 2\ell + 1$ resulting spectra. In addition, we multiply all power spectra by the relevant time duration in seconds. This arises from the definition of a temporal Fourier transform; the result represents so called power spectral density, and it takes care of

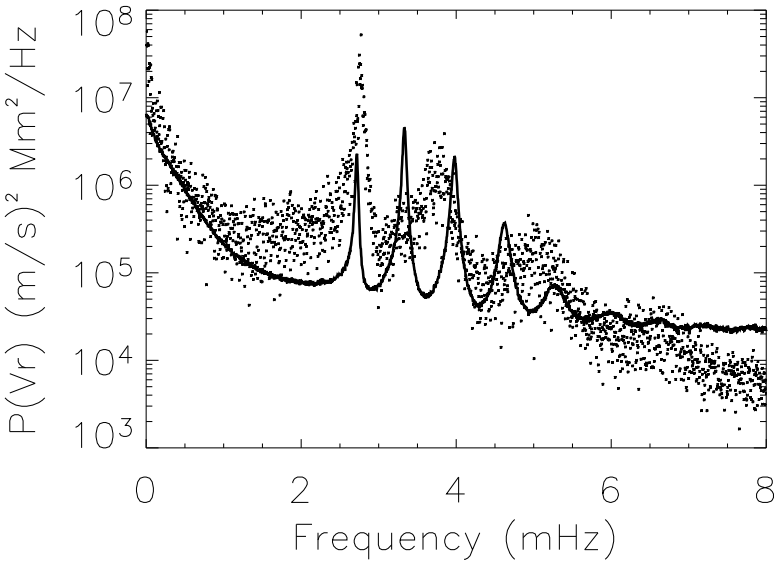

FIGURE 1. Power spectral density of vertical velocity in simulations (dots) and Doppler velocity in full disk observations (solid line) for angular degree $\ell = 740$.

different time duration and cadence between various data. We call the resulting power spectral densities, "power spectra", for brevity. The power spectra are also multiplied by an area over which the velocity measurements take place; this comes from the definition of a spatial Fourier transform. The result represents the oscillation power in this area.

5. Results

We start by reproducing the results of our earlier work (Georgobiani *et al.* (2000)). Figure 1 shows two power spectra of $\ell = 740$ modes, from simulations and the full-disk observations. One can see that the observed and simulated modes have similar amplitudes, but different mode structure, frequencies and mode widths. Also, the simulated power falls off more rapidly at high frequencies than the observed one.

Next, we compare the simulated power spectra with the high-resolution SOHO/MDI data. The results of comparison between the simulated and observed power spectra for $\ell = 740$ are presented in Fig 2, and for $\ell = 1480$ in Fig 3. Fig 2 is reminiscent of our earlier results (Fig 1). Fig 3, for $\ell = 1480$, shows remarkable similarity between simulations and observations in mode frequencies, amplitudes and widths, except for differences in the background noise level at low frequencies, away from modal structure. It is worth mentioning that the leftmost peak in all figures corresponds to the surface gravity (f) mode, while the others correspond to acoustic (p) modes. Frequencies of f-modes are independent of the depth of a resonant cavity, this is why even for $\ell = 740$ the f-mode peaks have the same frequency in simulations and observations. We sum over four individual spectra, because all of them contribute to the total power. In the full-disk data, we also need to sum over all m spectra when calculating the total power.

In Fig 4, we compare the two sets of our observational data, namely, high-resolution

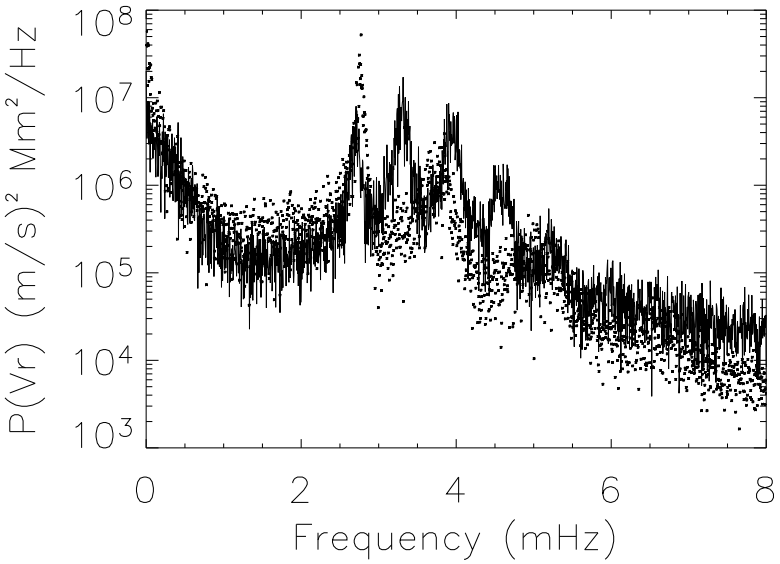

FIGURE 2. Power spectral density of vertical velocity in simulations (dots) and Doppler velocity in high-resolution observations (solid line) for angular degree $\ell = 740$. Amplitudes are similar, but frequencies and mode widths differ.

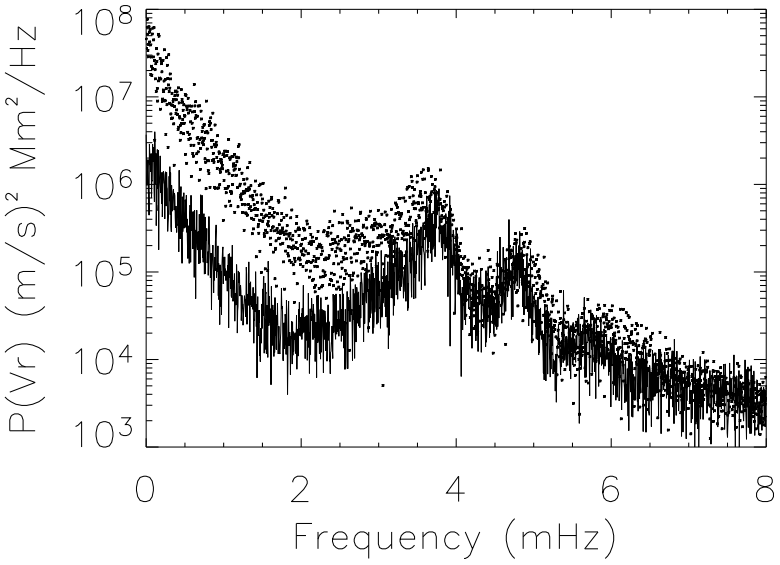

FIGURE 3. Power spectral density of vertical velocity in simulations (dots) and Doppler velocity in high-resolution observations (solid line) for angular degree $\ell = 1480$. There is a good correspondence between the two spectra, except at low frequencies.

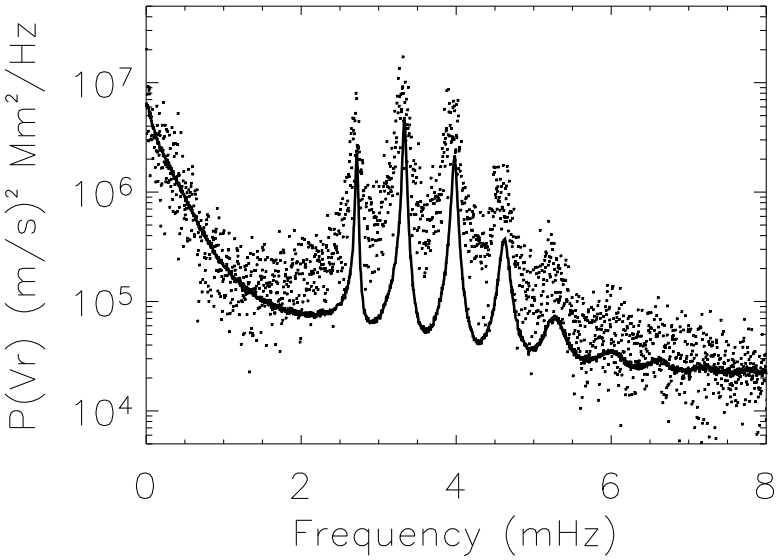

FIGURE 4. Power spectral density of Doppler velocity in the full-disk (solid line) and high-resolution (dots) observations for $\ell = 740$. Background and mode amplitudes are lower in the full-disk data, possibly because of the broad modulation of the high-resolution spectrum by leaking modes of various ℓ.

and full-disk measurements, for $\ell = 740$ (remember that we do not have $\ell = 1480$ full-disk data because of insufficient resolution of the full-disk MDI images). We perform similar comparison for $\ell = 370$ in Fig 5. The overall amplitudes of these spectra match rather well. The high-resolution spectra are much noisier than the full-disk spectra, because there are only four individual spectra to sum over, comparing to the superposition of $2\ell + 1 = 1481$ spectra in the full-disk data (cf also Fig 1). Averaging many spectra for individual m significantly decreases the noise level.

Finally, in Fig 6, we compare the two sets of full-disk spectra for $\ell = 370$ and 740. In this case, the background level became similar after the power spectra were multiplied by the inverse squared wavelength of the modes. Note that regardless of scaling, the mode amplitudes with respect to the background are somewhat smaller for larger ℓ.

6. Discussion

We find that for fully captured modes where the lower turning point is located inside the simulation domain, the simulated and observed vertical velocity power spectra are very similar, with similar amplitudes and line widths. Solar acoustic mode amplitudes are directly proportional to the excitation rate and inversely proportional to the mode damping rate. It has been shown by Stein & Nordlund (2001) that the simulated excitation rates are similar to the observed rates. The close match of the simulated and observed amplitudes, and especially mode line widths, suggests that the mode damping rates are also modeled properly by our simulation code, thus one can study the damping effects using the simulation data.

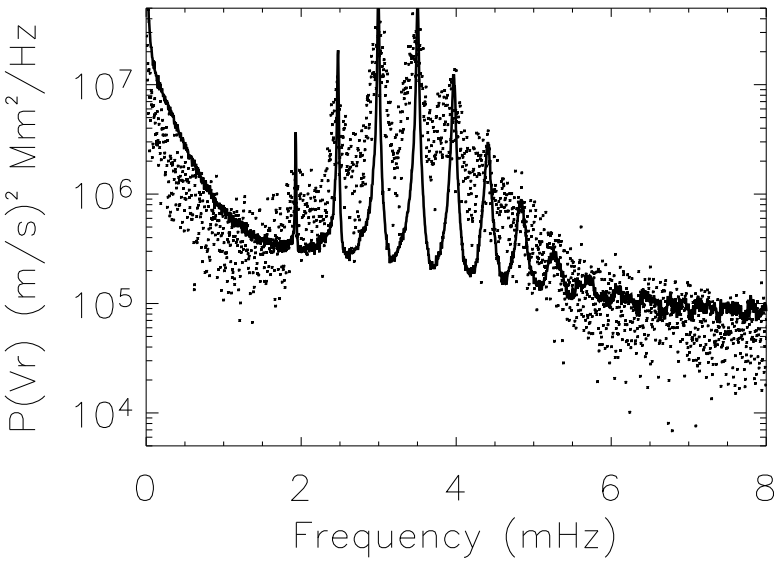

FIGURE 5. Power spectral density of Doppler velocity in the full-disk (solid line) and high-resolution (dots) observations for $\ell = 370$.

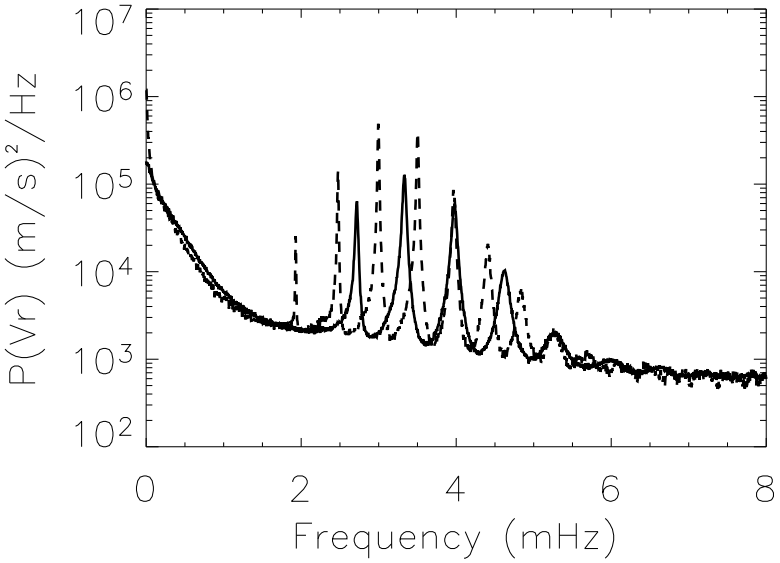

FIGURE 6. Power spectral density of Doppler velocity in the full-disk observations for $\ell = 740$ (solid line) and $\ell = 370$ (dashed line), normalized by oscillation area (6×6 and 12×12 Mm^2, respectively). Backgrounds are similar, while mode amplitudes are lower for higher ℓ.

Comparing the observed power spectra from high-resolution and full-disk data (Figs 4 and 5), we notice a broad overall peak in the high-resolution data (the mode peaks seem to be raised above the background), which is absent in the full-disk spectrum. The high-resolution spectrum calculated for a small area contains all the modes from radial to high degree, and the broad peak results from a superposition of all these modes. Apparently, the spherical transform method singles out individual ℓ modes better, although some inevitable leakage of neighboring modes is always present. In the simulation box, the horizontal boundaries are periodic, and thus the modes are far more discrete than in the patch of the real Sun.

Scaling of the power spectra of the full-disk data at different ℓ (Fig 6) with the square of the corresponding wavelength and resulting similarity between their backgrounds suggests that the background noise amplitudes (but not necessarily the mode amplitudes) of different ℓ scale with the area occupied by oscillations of a particular degree.

7. Future plans

We have compared the simulated and observed vertical velocity power spectral densities for solar oscillations of different angular degrees. We have found that there is a very good agreement between the oscillation frequencies and mode line widths when the mode radial eigenfunctions are completely contained in the simulation domain. These results, together with earlier findings about the similarity between the observed and simulated mode excitation rates, enable us to study excitation and damping mechanisms in more details. We have shown that the oscillation amplitudes in the observed and simulated data can be compared directly. In the future, similar simulations will be used to predict oscillation amplitudes and lifetimes for other stars.

Also, we have found that the power spectra for modes of different angular degree within the same data sets scale with the inverse square of their characteristic horizontal wavelength. This result is particularly prominent for the full disk solar data. It also holds for the low frequency part of the simulated power spectra, while the high-resolution power spectra do not show a clear scaling. We plan to investigate the cause of this relation between the spectra of different angular degree.

REFERENCES

GEORGOBIANI, D., KOSOVICHEV, A. G., NIGAM, R., NORDLUND, Å., & STEIN, R. F. 2000 Numerical Simulations of Oscillation Modes of the Solar Convection Zone. *Astrophysical Journal*, **530**, L139

NORDLUND, Å. & STEIN, R. F. 1990 3-D Simulations of Solar and Stellar Convection and Magnetoconvection. *Computer Physics Communications*, **59**, 119

STEIN, R. F. & NORDLUND, Å. 2000 Realistic Solar Convection Simulations. *Solar Physics*, **192**, 91

STEIN, R. F. & NORDLUND, Å. 2001 Solar Oscillations and Convection. II. Excitation of Radial Oscillations. *Astrophysical Journal*, **546**, 585